Available online at www.sciencedirect.com
ScienceDirect
Comparative Biochemistry and Physiology, Part C 144 (2007) 319–326
CBP
www.elsevier.com/locate/cbpc

Donepezil is a strong antagonist of voltage-gated calcium and potassium channels in molluscan neurons

Elena I. Solntseva, Julia V. Bukanova *, Evgeny Marchenko, Vladimir G. Skrebitsky

Brain Research Institute, Russian Academy of Medical Sciences, Per.Obukha,5, 105064, Moscow, Russia

Received 22 June 2006; received in revised form 4 October 2006; accepted 15 October 2006
Available online 19 October 2006

Abstract

Donepezil is an acetylcholinesterase inhibitor used in Alzheimer's disease therapy. The neuroprotective effect of donepezil has been demonstrated in a number of different models of neurodegeneration including beta-amyloid toxicity. Since the mechanisms of neurodegeneration involve the activation of both Ca^{2+}- and K^+-channels, the study of donepezil action on voltage-gated ionic currents looked advisable. In the present study, the action of donepezil on voltage-gated Ca^{2+}- and K^+-channels was investigated on isolated neurons of the edible snail (*Helix pomatia*) using the two-microelectrodes voltage-clamp technique. Donepezil rapidly and reversibly inhibited voltage activated Ca^{2+}-current (I_{Ca}) (IC_{50}=7.9 μM) and three types of high threshold K^+-current: Ca^{2+}-dependent K^+-current (I_C) (IC_{50}=6.4 μM), delayed rectifier K^+-current (I_{DR}) (IC_{50}=8.0 μM) and fast transient K^+-current (I_{Adepol}) (IC_{50}=9.1 μM). The drug caused a dual effect on low-threshold fast transient K^+-current (I_A), potentiating it at low (5 μM) concentration, but inhibiting at higher (7 μM and above) concentration. Donepezil also caused a significant hyperpolarizing shift of the voltage–current relationship of I_{Ca} (but not of any type of K^+-current). Results suggest the possible contribution of the blocking effect of donepezil on the voltage-gated Ca^{2+}- and K^+-channels to the neuroprotective effect of the drug.

Keywords: Cholinesterase inhibitor; Donepezil (E2020); Ca^{2+}-channel; K^+-channel; Molluscan neurons

1. Introduction

The role of ionic channels in the pathogenesis of Alzheimer's disease (AD) is a question of interest which is widely debated in literature. The absence of a distinct type of K^+-channels was found in fibroblasts from AD patients (Etcherberrigaray et al., 1993), and up-regulation of Kv3.4 K^+-channels subunit was discovered in the early stage of AD (Angulo et al., 2004).

Both Ca^{2+}- and K^+-channels are involved in the mechanisms of neurodegeneration induced by β-amyloid peptide (Abeta), which is the main component of neurotic plaques and is believed to play a critical role in the pathophysiology of AD. It was shown in mouse hippocampal neurons (Rovira et al., 2002) and cultured cortical neurons (Ba et al., 2004; MacManus et al., 2000) that Abeta-induced apoptosis was forestalled by the activation of voltage-gated Ca^{2+}-current (I_{Ca}), and Ca^{2+}-channels antagonist blocked Abeta-induced cell death (Ba et al., 2004). Another possible mechanism for Abeta-induced Ca^{2+}-dependent apoptosis is the blockade of fast-inactivating K^+-current (I_A). Such blockade was observed in rat hippocampal neurons and considered to lead to increase Ca^{2+}-influx via prolonging cell depolarization (Good et al., 1996; Xu et al., 1998).

Abeta-evoked neurodegenaration can also be governed by disturbances in K^+-homeostasis. The enhancement of slow-inactivating K^+-current (I_{DR}) followed by cellular K^+-loss and cell death was observed in cortical neurons (Yu et al., 1998), a cholinergic septal cell line (Colom et al., 1998), and in microglia (Chung et al., 2001) as affected by Abeta. Reducing I_{DR} by adding the K^+-channel blocker tetraethylammonium (TEA) attenuated Abeta-induced neuronal death, while the I_A blocker 4-aminopyridine (4-AP) was not neuroprotective (Yu et al., 1998).

This data raises the possibility that manipulations aimed at reducing I_{Ca} and I_{DR} may provide an approach to reducing neuronal degeneration in patients with AD.

Donepezil is a potent acetylcholinesterase inhibitor(AChEI) used for treatment of AD (Standridge, 2002). Perhaps, other mechanisms of its action than AChE inhibition exist. The

* Corresponding author.
E-mail address: bukanovaj@mail.ru (J.V. Bukanova).

1532-0456/$ - see front matter © 2006 Elsevier Inc. All rights reserved.
doi:10.1016/j.cbpc.2006.10.001

neuroprotective effect of donepezil has been demonstrated in a number of different models (Akasofu et al., 2003, 2006; Takada et al., 2003; Zhou et al., 2001) including Abeta-toxicity (Arias et al., 2005; Kimura et al., 2005). Therefore, donepezil is expected to have a protective effect against progressive degeneration of brain neuronal cells in AD (Akasofu et al., 2003). Since mechanisms of neurodegenaration are believed to involve the activation of voltage-gated Ca^{2+}- and/or K^+-channels, the study of the effect of donepezil on these channels looks promising. The influence of donepezil on voltage-gated K^+-currents were studied in rat hippocampal neurons by two groups of investigators (Yu and Hu, 2005; Zhong et al., 2002), and the results did not coincide completely. Zhong et al. (2002) observed the inhibition of delayed rectifier K^+-current (I_{DR}) by donepezil at concentration as low as 1 μM, while Yu and Hu (2005) have found that rather high concentrations of the drug are required to block both I_{DR} ($IC_{50}=78\pm5$ μM) and I_A ($IC_{50}=249\pm25$ μM). Because of the high concentration required, Yu and Hu have concluded that the blocking effects of donepezil on K^+-channels are unlikely to contribute to the clinical improvement in patients with AD. As for the inward I_{Ca}, the effect of donepezil on this current was not examined yet.

The goal of the present work was to study the effects of donepezil on high threshold I_{Ca} and four types of voltage-gated K^+-currents using the model of the molluscan neuron. In molluscan neurons, voltage-gated Ca^{2+}- and K^+-currents have been extensively characterized. High threshold I_{Ca} was identified as L-type-like Ca^{2+}-current (White and Kaczmarek, 1997). High threshold K^+-currents were resolved into three distinct components that include: I_{DR}, a slow-inactivating, TEA-sensitive current; I_C, slow-inactivating, Ca^{2+}-activated K^+-current, which is also TEA-sensitive; and I_{Adepol}, a high threshold, fast-inactivating, 4-AP-sensitive current (Bal et al., 2001; Baxter and Byrne, 1989; Thompson, 1977). Low threshold transient K^+-current (I_A) was also described in molluscan neurons (Bal et al., 2001; Furukawa et al., 1992). This current is inactivated at the resting membrane potential but can be activated at subthreshold potentials after a hyperpolarizing prepulse, which removes the inactivation. The properties of Ca^{2+}- and K^+-currents in molluscan neurons look similar, in general, to the properties of corresponding currents in mammalian neurons (Catterall, 1995; Jeziorski et al., 2000; Kaczorowski and Garcia, 1999).

2. Materials and methods

2.1. Reagents

Donepezil solutions were prepared by dissolving tablets of *Aricept* (Pfizer) containing 5 mg of donepezil hydrochloride. A tablet was dissolved in extracellular solution. The liquid was filtered using membrane filter with 0.45 μM pore diameter (Schleicher and Schul), so that insoluble ingredients (corn starch, microcrystalline cellulose, magnesium stearate, talk) were filtered out. Then the drug solution was introduced to the working chamber at stopped flow. TEA and 4-AP were purchased from Sigma.

2.2. Cell isolation

The experiments were performed on isolated neurons of the visceral ganglion and the left and right parietal ganglions of the land snail (*Helix pomatia*). Neurons were isolated with the help of perfect needles without any pretreatment of the ganglia with proteolytic enzymes. The neurons were pipetted into the recording chamber of about 1 mL volume and were continuously perfused with a standard Ringer solution feeding by gravity.

2.3. Voltage clamp

Two microelectrodes voltage-clamp technique was used. The microelectrodes were filled with potassium citrate solution (2 M) and had a tip resistance of 12–14 MΩ. The experiments were performed using a MEZ 7101 micro-electrode amplifier and a CEZ 1100 voltage-clamp amplifier (Nihon Kohden, Japan). Voltages and currents were recorded using a RJG 4024 four-channel pen-recorder with a bandwidth of up to 40 kHz. High-threshold Ca^{2+}- and high threshold K^+-currents were triggered by depolarizing test pulses from the holding potential of −60 and −50 mV, correspondingly. To study the low-threshold K^+-current (I_A), depolarizing test pulses were applied from the holding potential of −130 mV. In tracing the *I–V* curves, the current responses to equivalent hyperpolarizing pulses were added to cancel linear leakage.

2.4. Experimental solutions

Voltage-gated K^+-currents were recorded in normal Ringer solution containing (in mM): NaCl 100, KCl 4, $CaCl_2$ 5, $MgCl_2$ 4, $NaHCO_3$ 3, Tris–Cl 5 (pH=7.6). Na^+-free solution containing K^+-channel antagonists was used when analyzing the Ca^{2+}-current. This solution was composed of (mM): KCl 4, $CaCl_2$ 10, $MgCl_2$ 4, TEA-Cl 95, 4-AP 5, Tris–Cl 5 (pH 7.6).

2.5. Data analysis

Statistical analysis was performed with the use of the Prism 3.0 (GraphPad) software. Group data is presented as mean±S.E.M. Statistical tests of drugs effects were performed using unpaired *t* test. A *t* value producing $P<.05$ was considered to be significant.

3. Results

3.1. Inhibitory effect of donepezil on voltage-activated calcium current in molluscan neurons

High-threshold Ca^{2+} currents (I_{Ca}) were triggered by depolarizing 150–500 ms test pulses applied from the holding potential of −60 mV. Test pulses varied from −30 to +60 mV with increments of 10 mV. The maximal I_{Ca} was observed at the potential 30–40 mV. Application of 1–100 μM donepezil caused a rapid, reversible and dose-dependent reduction of the maximal I_{Ca} ($n=6/6$). The effect reached a maximum in 1–3 min after

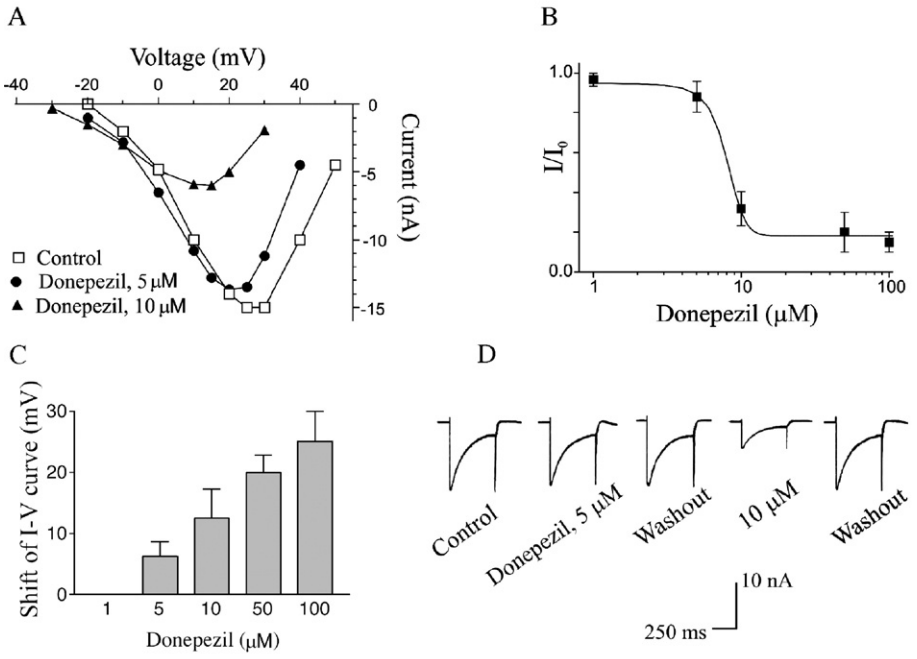

Fig. 1. Inhibitory effect of donepezil on voltage-gated calcium current in molluscan neurons. Ca^{2+}-current was recorded in Na^{+}-free solution, containing 95 mM TEACl and 5 mM 4-AP. (A) The *I–V* relationships for peak inward current, constructed before and during application of 5 or 10 μM donepezil. (B) Dose–response curve of donepezil effect on the maximal I_{Ca} amplitude. The normalized mean amplitude of maximal I_{Ca} is plotted vs. logarithmic concentration of donepezil. Each value represents the mean of six cells. Sigmoid curve was generated using Boltzmann equation. (C) Dependence of the hyperpolarizing shift of the maximal I_{Ca} on donepezil concentration. Each column is the mean ± S.E.M. ($n=6$). (D) Current traces recorded in control solution and in the presence of 5 or 10 μM donepezil. The recordings were obtained from the same neuron as in (A). The neuron was held at −60 mV and depolarizing step of 500 ms was applied. The pulse amplitude was chosen to elicit the maximal current (to 30 mV in normal solution (control, washout), to 25 mV in the presence of 5 μM donepezil, or to 15 mV in the presence of 10 μM donepezil).

drug application, and was washed out in 6–8 min. Fig. 1A shows the current–voltage (*I–V*) curves of the inward I_{Ca} constructed in control solution and in the presence of 5 or 10 μM of donepezil in one of the cells examined. Donepezil caused both a decrease in the amplitude of maximal I_{Ca} and a hyperpolarizing shift of the *I–V* curve. The maximal I_{Ca} in the presence of 5 and 10 μM donepezil shifted by 5 and 15 mV, accordingly. Fig. 1B shows dose–effect relationship for inhibition of maximal I_{Ca} by donepezil. The effect of 5 μM donepezil was not significant (by 12.2 ± 8.5%, $P>0.05$), whereas 10 μM donepezil suppressed I_{Ca} by 67.6 ± 15.7% ($P<0.005$). The maximal inhibition of I_{Ca} was 81.7 ± 9.3%, $P<0.001$ when donepezil was at 100 μM. Data was fitted with sigmoidal curve generated using the Boltzman equation. Analysis of the concentration–response relationship revealed an IC_{50} value of 7.9 μM, with a slope factor (Hill coefficient) of 1.1. Fig. 1C shows the dependence of the hyperpolarizing shift of the maximal I_{Ca} on donepezil concentration. The maximal shift value reached to 24.0 ± 3.7 mV ($P<0.001$) when donepezil was at 100 μM. The kinetics of the fast activation and inactivation of I_{Ca} was not changed significantly in the presence of donepezil as seen from original current recordings shown in Fig. 1D.

3.2. Different types of high threshold potassium current in different cells

High-threshold potassium currents were evoked by depolarizing test pulses of 150–500 ms applied from the holding potential of −50 mV. Test pulses varied from −30 to +100 mV with increments of 10 mV. The threshold of potassium current activation was near −20 mV. It was found that outward K^{+}-current varied in different cells by kinetics of activation and inactivation, shape of the *I–V* curve and sensitivity to antagonists. In one group of the cells, the outward current had slow gate kinetics, demonstrated the N-shaped *I–V* curve (Fig. 2) and was insensitive to 1 mM 4-AP, but was almost completely blocked by 1 mM TEA. The *I–V* curve became smooth in Ca^{2+}-free solution, suggesting that the N-shape of this curve was due to a summation of Ca^{2+}-dependent (I_C) and Ca^{2+}-independent (I_{DR}) components. In another group of cells, K^{+}-current showed fast kinetics of activation and inactivation, had a smooth *I–V* curve (Fig. 3) and was blocked by 1 mM 4-AP but not by TEA (I_{Adepol}). Our results agree with literature data distinguishing I_C, I_{DR}, and I_{Adepol} in molluscan neurons (Bal et al., 2001; Baxter and Byrne, 1989; Thompson, 1977). To exclude the possible contamination of slow-inactivating K^{+}-currents (I_C and I_{DR}) with I_{Adepol}, 1 mM 4-AP was added to the control solution. Accordingly, 1 mM TEA was added to bath medium when I_{Adepol} was studied.

3.3. Strong blockade of slow-inactivating K^{+}-currents (I_C and I_{DR}) by donepezil

Donepezil, used at concentration of 1–100 μM, caused a fast, reversible and dose-dependent reduction of the amplitude of slow-inactivating K^{+}-current recorded at all test potentials ($n=9/9$) (Fig. 2A–C). The effect reached a maximum 1–3 min

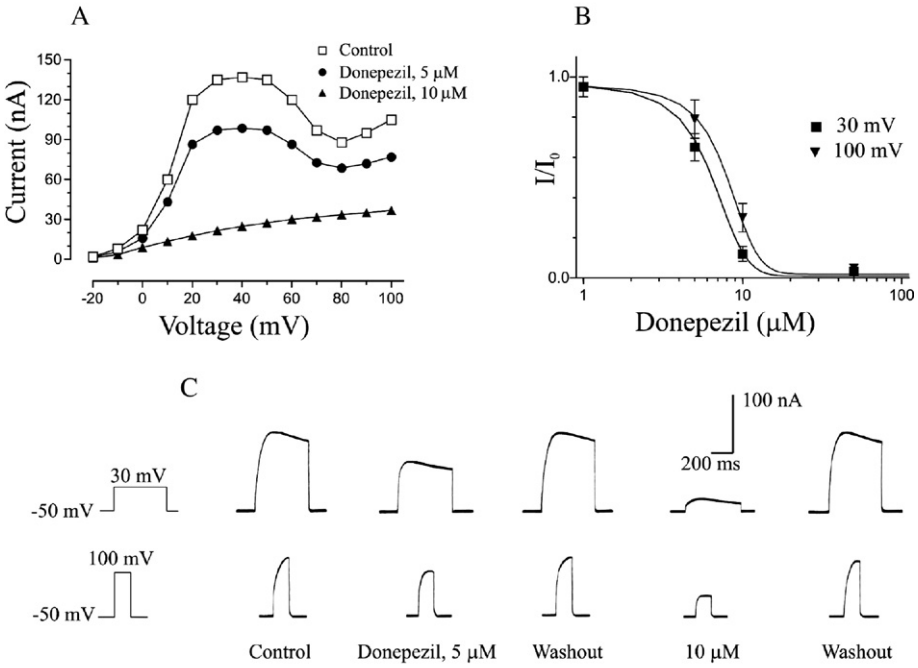

Fig. 2. Strong inhibitory effect of donepezil on slow-inactivating potassium current. The current was recorded in Ringer solution, containing 1 mM 4-AP. (A) Current–voltage relationships for peak outward current, constructed in normal solution and in the presence of 5 or 10 μM donepezil are shown. (B) Dose–response curves of blocking effect of donepezil on the peak amplitude of slow-inactivating outward current recorded at 30 mV and 100 mV. The normalized mean amplitude of outward current is plotted vs logarithmic concentration of donepezil. Each value represents the mean±S.E.M. of nine cells. Data were fitted with Boltzmann function. (C) Original current recordings obtained in control solution, 5 min after the application of 5 or 10 μM donepezil and after washout of the drug. The recordings were obtained from the same neuron as in (A). The neuron was held at −50 mV. The upper traces show the currents elicited with a 500 ms depolarizing step to 30 mV. The lower traces demonstrate the currents evoked by a 150 ms depolarizing step to 100 mV. Test pulses are shown on the left from current recordings.

after the drug application and wholly disappeared after 6–8 min of washing. Fig. 2A shows the *I–V* curves of slow-inactivating K^+-current in one of the cells. The outward current within the potential range from −20 mV to 70 mV was provided essentially by I_C with little contamination with I_{DR}, while in the range 80–100 mV, it was composed of only the I_{DR}. Maximal I_C was observed at +30 mV, while maximal I_{DR} was recorded at highest test potential applied (+100 mV). The *I–V*

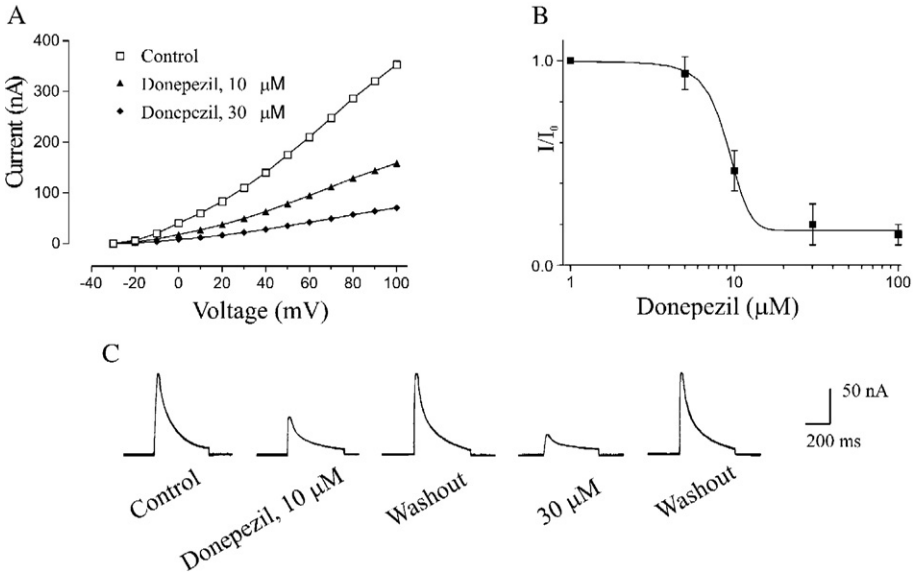

Fig. 3. Moderate blockade of high threshold transient K^+-current (I_{Adepol}) by donepezil. I_{Adepol} was recorded in solution, containing 1 mM TEACl. (A) Current–voltage relationship for peak outward current in control solution and in solutions containing 10 or 30 μM donepezil. (B) Dose–response curve of inhibiting effect of donepezil on the peak amplitude of fast inactivating outward current recorded at 30 mV. Each value represents the mean of eight cells. Continuous line shows best fit with Boltzmann equation. (C) The representative I_{Adepol} traces in control solution, during application of 10 or 30 μM donepezil and after washout of the drug. The currents elicited with a 500 ms depolarizing step to 30 mV applied from a −50 mV holding potential. The recordings were obtained from the same neuron as in (A).

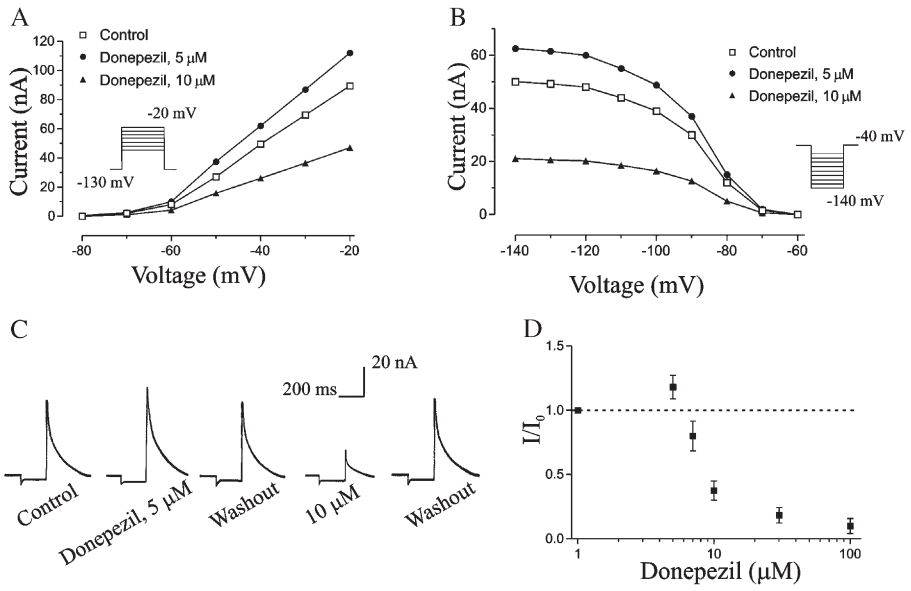

Fig. 4. Dual effect of donepezil on the low-threshold transient K^+-current (I_A). (A) Current–voltage relationship for peak outward current in control solution and in the presence of 5 or 10 μM donepezil. The neuron was held at −130 mV and a series of 150–500 ms steps from −80 to −20 mV with 10 mV increment was applied. The inset shows the protocol of cell stimulation. (B) Steady-state inactivation curve for the I_A from the same cell as shown in (A). The current was measured at −40 mV after a prepulse of 200 ms hyperpolarizing membrane from −140 mV to −60 mV with 10 mV increments. (C) Outward currents recorded at −40 mV after 200 ms prepulse to −130 mV. The currents were registered in control solution, during application of 5 or 10 μM donepezil and after washout of the drug (the same cell as shown in A and B). (D) Dose–response relationship of donepezil effect on the peak amplitude of the I_A measured at −40 mV after 200 ms hyperpolarizing prepulse to −130 mV. Each value represents the mean of five cells.

curves constructed in the presence of 5 and 10 μM donepezil indicate that K^+-current was suppressed effectively at both 30 and 100 mV. Unlike Ca^{2+}-current, no shift of the *I–V* curve of the K^+-current along the potential axis was observed in the presence of the drug. Dose–effect relationships of donepezil inhibition of K^+-currents recorded at 30 mV (I_C) and 100 mV (I_{DR}) are shown in the Fig. 2B. The I_C amplitude was decreased by 5, 10 and 50 μM donepezil to 65.0±6.7%, ($P<0.001$), 12.9± 3.4% ($P<0.0001$) and 3.1±2.7% ($P<0.0001$), accordingly. The I_{DR} amplitude was suppressed by the same concentrations of the drug to 79.1±9.5% ($P>0.05$, ns), 30.1±7.2% ($P<0.001$) and 4.5±0.5% ($P<0.0001$). Continuous lines show best fits with the Boltzmann equation. The IC_{50} values for blocking effect at 30 mV and at 100 mV were calculated as 6.4 μM and 8.0 μM, accordingly, with the Hill slopes of 1.8 and 2.0, correspondingly. The decrease in the amplitude of the K^+-current was not accompanied by the change of the kinetics of activation/inactivation in 5 out of 9 neurons (Fig. 2C). In other 4 cells, however, the application of donepezil caused both a reduction in the peak current amplitude and an acceleration of the current decay (not shown).

3.4. Moderate blockade of high threshold transient K^+-current (I_{Adepol}) by donepezil

Donepezil caused a reversible and dose dependent inhibition of the I_{Adepol}, although this current appeared to be less sensitive to the drug than slow-inactivating K^+-current. Fig. 3A illustrates the *I–V* relationships of I_{Adepol} constructed before and during application of 10 and 30 μM donepezil. One can see that donepezil causes voltage-independent inhibition of the I_{Adepol}, without shifting the *I–V* curve along voltage axis. Dose–effect relationship of donepezil inhibition of the I_{Adepol} recorded at 30 mV is shown in Fig. 3B ($n=8$). The current amplitude values decreased to 92.5±7.1% and 47.3±11.4% in the presence of 5 and 10 μM donepezil, accordingly. These values were larger significantly ($P<0.05$) than corresponding quantities for I_C. The IC_{50} and the slope factor (Hill coefficient) were 9.1 μM and 1.5, respectively. Fig. 3C shows original recordings of the I_{Adepol}. No obvious changes of the kinetic properties of the current could be observed after donepezil application.

3.5. Dual effect of donepezil on the low-threshold transient K^+-current (I_A)

The I_A is inactivated at the resting membrane potential. To reveal this current, a hyperpolarizing pulse must be applied for removal of inactivation. To construct *I–V* curve, the cell was held at −130 mV, and the command pulses to potentials from −80 to −20 mV were applied in increments of 10 mV (Fig. 4A). To avoid the contamination with high-threshold currents, we did not study I_A at potentials above −20 mV. The I_A activation threshold was found to be near −70 mV. To examine the steady-state inactivation of I_A, the cell was held at −40 mV and 200 ms hyperpolarizing prepulses to potentials from −60 mV to −120 mV (in 10 mV increments) were applied. The outward current was measured at −40 mV after these hyperpolarizing prepulses. (Fig. 4B and C). Donepezil appeared to cause a dual effect on the I_A depending on concentration. At low concentration (5 μM) the drug reversibly augmented I_A whereas at concentrations above 7 μM it inhibited this current. The dual effect of donepezil can be observed on both the *I–V* curve and the steady-state inactivation curve, as it is

shown on Fig. 4A and B. Both effects were voltage-independent. Fig. 4D shows the dose–response curve for donepezil effects on I_A elicited at 30 mV. The I_A amplitude was augmented to 116.7±9.2% by 5 μM donepezil, but was inhibited to 40.2±6.3% ($P<0.0001$) or 7.2±4.8% ($P<0.0001$) by 10 or 100 μM donepezil, accordingly.

3.6. Control experiments with lactose

Tablets of "Aricept" contain both insoluble and soluble ingredients as inert filling materials. While insoluble ingredients were filtered out, soluble ingredients contaminated donepezil solution. Lactose was the main soluble ingredient of the inert filling material. We measured both Ca^{2+}- and different types of K^+-current of molluscan neurons in the presence of lactose (ChemMed, Russia) in the wide range of concentrations, and found no noticeable effects.

4. Discussion

In the present study, strong blocking effects of donepezil on voltage-gated calcium and potassium currents of molluscan neurons are described.

This study is the first demonstration of donepezil influence on the voltage-gated Ca^{2+}-channel. The application of donepezil caused rapid, reversible and dose-dependent inhibition of the I_{Ca} amplitude ($IC_{50}=7.9$ μM) suggesting direct interaction of the drug with the Ca^{2+}-channel. The Hill coefficient was close to 1, indicating the absence of cooperation between binding sites. Besides the reduction of I_{Ca} amplitude, the hyperpolarizing shift of the *I–V* curve was observed in the presence of donepezil suggesting the occurrence of some changes in the surface charge density. In literature, Ca^{2+}-channel blocking activity was described for some other AChEIs that are considered to be possible drug candidates for AD therapy. These include alkaloid juliflorin in rabbit jejunum preparations (Choudhary et al., 2005), a new series of tacrine derivates in bovine adrenal chromaffin cells (de los Rios et al., 2002), and a carbamate-type AChEI in guinea pig ventricular myocytes (Futagawa et al., 2002). The blockade of voltage-gated Ca^{2+}-channel seems to be a desirable pharmaceutical property for AD therapy because an increase in cytosolic Ca^{2+} was shown to contribute to neuronal degeneration in AD. It has been well documented that Abeta which is thought to underlie the neurodegeneration in AD, potentiates the voltage-gated Ca^{2+}-channel (Ekinci et al., 1999; MacManus et al., 2000; Rovira et al., 2002). The inhibition of the I_{Ca} by donepezil shown in the present work might be involved in mechanisms of the neuroprotective effect of the drug.

Our next results concern the influence of donepezil on voltage-gated K^+-currents of molluscan neurons. Donepezil caused an inhibitory effect on three types of high threshold K^+-current: I_C ($IC_{50}=6.4$ μM), I_{DR} ($IC_{50}=8.0$ μM) and $I_{Adepoil}$ ($IC_{50}=9.1$ μM). As I_C is a Ca^{2+}-dependent current, its inhibition by donepezil can be explained by I_{Ca} suppression.

However, 5 μM donepezil reduced I_C significantly stronger than I_{Ca}, (35.0±7.2% *versus* 12.2±8.5%, $P<0.05$), suggesting that mechanisms of I_C inhibition may be independent of Ca^{2+}-channels blockage. The Hill coefficients for all three types of K^+-currents were bigger than 1, indicating positive cooperation between binding sites. Unlike I_{Ca}, no shift of the *I–V* curves for K^+-currents along the potential axis was observed.

The IC_{50} values for K^+-currents calculated in our experiments were much lower than those drawn by Yu and Hu (2005) in rat hippocampal neurons using a patch clamp technique. In their study, the IC_{50} values for the blocking action of donepezil on delayed rectifier K^+-current was 78 μM, and on fast transient K^+-current was 249 μM. The reasons for this incongruity may be due to the differences between i) models (molluscan versus rat neurons), and ii) methods (two-microelectrodes voltage clamp versus whole cell patch clamp). The idea about evolutionary conservation of ionic channel proteins is widely accepted (Catterall, 1995; Kaczorowski and Garcia, 1999). However, amino-acid sequence identity of channel protein across the species is high, but not complete. For example, ~70% of the amino acids in A-type K^+-channels in neurons of the mollusc *Aplysia* was shown to be identical to *Shaker* K^+-channels clones from other species (Pfaffinger et al., 1991). A sequence identity of 61% was found for *Drosophila* and rat *eag*-type K^+-channels (Ludwig et al., 1994). These structural differences (although, not large) between K^+-channels from different animals seem to be the basis for essential species diversity of the pharmacological properties of K^+-channels (Restano-Cassulini et al., 2006). Another reason for lower sensitivity of K^+-currents to donepezil observed by Yu and Hu, may be due to peculiarities of patch clamp method, which comprise dialysis of the neuron and may cause disturbances in phosphorylation/dephosphorylation processes and changes in channel properties. We used thin microelectrodes which did not damage the cytoplasm as much, and channels functions were believed to be more approximated to physiological conditions.

In our study, we also found that donepezil caused a dual effect on low-threshold transient K^+-current (I_A). Low concentration of the drug (5 μM) potentiated the current, whereas higher concentrations (7 μM and above) inhibited it. The mechanism of I_A potentiation by low-dose donepezil remains to be elucidated. One may suggest that this effect can involve some metabolic pathways. The ability of donepezil to interfere with cellular metabolism is supported by the findings by Borroni et al. (2001) indicating that the drug modifies the ratio of different forms of amyloid precursor protein in platelets in AD. Furthermore, donepezil has been shown to be a potent agonist of the sigma1 receptor (Maurice et al., 2006), which is known to govern several biochemical processes. Interestingly, earlier we found the potentiation of I_A of molluscan neurons by another cognitive enhancer, vinpocetine, and an involvement of cyclic GMP cascade was strongly suggested for the mechanism of this potentiation (Solntseva et al., 2001).

A stronger blocking effect of donepezil on the slow-inactivating K^+-current (I_C and I_{DR}) than on the fast-inactivating K^+-current (I_{Adepol} and I_A) described in our work is in accordance with the results of other authors who studied the effects of AChEIs on K^+-currents. In rat hippocampal neurons, donepezil (Yu and Hu, 2005), galantamine (Pan et al., 2002) and rivastigmine (Pan et al., 2003) inhibit I_{DR} to a bigger extent than

I_A. Similarly, tacrine has been found to block I_{DR} without affecting I_A in larval muscle of *Drosophila* (Kraliz and Singh, 1997). In molluscan neurons, a similar tendency was detected in our earlier experiments for other cognitive enhancers: vinpocetine and piracetam (Bukanova et al., 2002). This pharmacological profile for cognitive enhancers does not seem accidental. Slow-inactivating K^+-channels were found to be a particularly sensitive target for Abeta. Exposure to Abeta-fragments enhances the I_{DR}, but does not affect the I_A in cortical neurons (Yu et al., 1998). I_{DR} reduction by TEA attenuated Abeta-induced neuronal death, whereas the I_A blocker 4-AP did not have a neuroprotective action.

Donepezil has been reported to have a neuroprotective effect against various apoptotic factors. The drug, used at concentrations of 0.1–10 μM, protected neurons against oxygen-glucose deprivation (Akasofu et al., 2003), glutamate neurotoxicity (Takada et al., 2003), NMDA toxicity (Akasofu et al., 2006) and Abeta toxicity (Arias et al., 2005; Kimura et al., 2005). Results of the present study suggest that the mechanism(s) of neuroprotective effects of donepezil may be explained, at least partially, by inhibition of voltage-gated Ca^{2+}- and/or K^+-currents.

Acknowledgment

This work was supported by Grant 07-04-00636 from the Russian Foundation for Basic Research.

References

Akasofu, S., Kosasa, T., Kimura, M., Kubota, A., 2003. Protective effect of donepezil in primary culture of rat cortical neurons exposed to oxygen-glucose deprivation. Eur. J. Pharmacol. 472, 57–63.

Akasofu, S., Kimura, M., Kosasa, T., Ogura, H., Sawada, K., 2006. Protective effect of donepezil in primary-cultured rat cortical neurons exposed to *N*-methyl-D-aspartate (NMDA) toxicity. Eur. J. Pharmacol. 530, 215–222.

Angulo, E., Noe, V., Casado, V., Mallol, J., Gomez-Isla, T., Lluis, C., Ferrer, I., Ciudad, C.J., Franco, R., 2004. Up-regulation of the Kv3.4 potassium channel subunit in early stage of Alzheimer's disease. J. Neurochem. 91, 547–557.

Arias, E., Gallego-Sandin, S., Villarroya, M., Garcia, A.G., Lopez, M.G., 2005. Unequal neuroprotection afforded by the acetylcholinesterase inhibitors galantamine, donepezil, and rivastigmine in SH-SY5Y neuroblastoma cells: role of nicotinic receptors. J. Pharmacol. Exp. Ther. 315, 1346–1353.

Ba, F., Pang, P.K., Benishin, C.G., 2004. The role of Ca^{2+} channel modulation in the neuroprotective actions of estrogen in beta-amyloid protein and 1-methyl-4-phenyl-1,2,3,6-tetrahydropyridine (MPTP) cytotoxic models. Neurochem. Int. 45, 31–38.

Bal, R., Janahmadi, M., Green, G.G., Sanders, D.J., 2001. Two kinds of transient outward currents, I_A and I_{Adepol}, in F76 and D1 soma membranes of the subesophageal ganglia of *Helix aspersa*. J. Membr. Biol. 179, 71–78.

Baxter, D.A., Byrne, J., 1989. Serotonergic modulation of two potassium currents in the pleural sensory neurons of *Aplysia*. J. Neurophysiol. 62, 665–679.

Borroni, B., Colciaghi, F., Pastorino, L., Pettenati, C., Cottini, E., Rozzini, I., Monastero, R., Lenzi, G.L., Cattabeni, F., Di Luca, M., Padovani, A., 2001. Amyloid precursor protein in platelets of patients with Alzheimer disease: effect of acetylcholinesterase inhibitor treatment. Arch. Neurol. 58, 442–446.

Bukanova, J.V., Solntseva, E.I., Skrebitsky, V.G., 2002. Selective suppression of the slow-inactivating potassium currents by nootropics in molluscan neurons. Int. J. Neuropsychopharmacol. 5, 229–237.

Catterall, W., 1995. Structure and function of voltage-gated ion channels. Annu. Rev. Biochem. 64, 493–531.

Choudhary, M.I., Nawaz, S.A., Zaheer-ul-Haq, Azim, M.K., Ghayur, M.N., Lodhi, M.A., Jalil, S., Khalid, A., Ahmed, A., Rode, B.M., Atta-ur-Rahman, Gilani, A.U., Ahmad, V.U., 2005. Juliflorine: a potent natural peripheral anionic-site-binding inhibitor of acetylcholinesterase with calcium-channel blocking potential, a leading candidate for Alzheimer's disease therapy. Biochem. Biophys. Res. Commun. 332, 1171–1177.

Chung, S., Lee, J., Joe, E.H., Uhm, D.Y., 2001. Beta-amyloid peptide induces the expression of voltage dependent outward rectifying K^+ channels in rat microglia. Neurosci. Lett. 300, 67–70.

Colom, L.V., Diaz, M.E., Beers, D.R., Neely, A., Xie, W., Appel, S.H., 1998. Role of potassium channels in amyloid-induced cell death. J. Neurochem. 70, 1925–1934.

de los Rios, C., Marco, J.L., Carreiras, M.D., Chinchon, P.M., Garcia, A.G., Villarroya, M., 2002. Novel tacrine derivatives that block neuronal calcium channels. Bioorg. Med. Chem. 10, 2077–2088.

Ekinci, F.J., Malik, K.U., Shea, T.B., 1999. Activation of the L voltage-sensitive calcium channel by mitogen-activated protein (MAP) kinase following exposure of neuronal cells to beta-amyloid. Map kinase mediates beta-amyloid-induced neurodegeneration. J. Biol. Chem. 274, 30322–30327.

Etcherberrigaray, R., Ito, E., Oka, K., Tofel-Grehl, B., Gibson, G.E., Alkon, D.L., 1993. Potassium channel dysfunction in fibroblasts. Proc. Natl. Acad. Sci. U. S. A. 90, 8209–8213.

Furukawa, Y., Kandel, E.R., Pfaifinger, P., 1992. Three types of early transient potassium currents in *Aplysia* neurons. J. Neurosci. 12, 989–1000.

Futagawa, H., Takahashi, H., Nagao, T., Adachi-Akahane, S., 2002. A carbamate-type cholinesterase inhibitor 2-*sec*-butylphenyl *N*-methylcarbamate insecticide blocks L-type Ca^{2+} channel in guinea pig ventricular myocytes. Jpn. J. Pharmacol. 90, 12–20.

Good, T.A., Smith, D.O., Murphy, R.M., 1996. β-amyloid peptide blocks the fast-inactivating K^+ current in rat hippocampal neurons. Biophys. J. 70, 296–304.

Jeziorski, M.C., Greenberg, R.M., Anderson, P.A.V., 2000. The molecular biology of inbvertebrate voltage-gated Ca^{2+} channels. J. Exp. Biol. 203, 841–856.

Kaczorowski, G.J., Garcia, M.L., 1999. Pharmacology of voltage-gated and calcium-activated potassium channels. Curr. Opin. Chem. Biol. 3, 448–458.

Kimura, M., Akasofu, S., Ogura, H., Sawada, K., 2005. Protective effect of donepezil against Abeta (1–40) neurotoxicity in rat septal neurons. Brain Res. 1047, 72–84.

Kraliz, D., Singh, S., 1997. Selective blockade of the delayed rectifier potassium current by tacrine in *Drosophila*. J. Neurobiol. 32, 1–10.

Ludwig, J., Terlau, H., Wunder, F., Bruggemann, A., Pardo, L.A., Marquardt, A., Stuhmer, W., Pongs, O., 1994. Functional expression of a rat homologue of the voltage gated either a go-go potassium channel reveals differences in selectivity and activation kinetics between the *Drosophila* channel and its mammalian counterpart. EMBO J. 13, 4451–4458.

MacManus, A., Ramsden, M., Murray, M., Henderson, Z., Pearson, H.A., Campbell, V.A., 2000. Enhancement of $^{45}Ca^{2+}$ influx and voltage-dependent Ca^{2+} channel activity by beta-amyloid-(1–40) in rat cortical synaptosomes and cultured cortical neurons. Modulation by the proinflammatory cytokine interleukin-1beta. J. Biol. Chem. 275, 4713–4718.

Maurice, T., Meunier, J., Feng, B., Ieni, J., Monaghan, D.T., 2006. Interaction with {sigma}1 protein, but not NMDA receptor, is involved in the pharmacological activity of donepezil. J. Pharmacol. Exp. Ther. 317, 606–614.

Pan, Y., Xu, X., Wang, X., 2002. Galantamine blocks delayed rectifier, but not transient outward potassium current in rat dissociated hippocampal pyramidal neurons. Neurosci. Lett. 336, 37–40.

Pan, Y., Xu, X., Wang, X., 2003. Rivastigmine blocks voltage-activated K^+ currents in dissociated rat hippocampal neurons. Br. J. Pharmacol. 140, 907–912.

Pfaffinger, P.J., Furukawa, Y., Zhao, B., Dugan, D., Kandel, E.R., 1991. Cloning and expression of an *Aplysia* K^+ channel and comparison with native *Aplysia* K^+ channel. J. Neurosci. 11, 918–927.

Restano-Cassulini, R., Korolkova, Y.V., Diochot, S., Gurrola, G., Guasti, L., Possani, L.D., Lazdunski, M., Grishin, E.V., Arcangeli, A., Wanke, E., 2006.

Species diversity and peptide toxins blocking selectivity of ether-a-go-go-related gene subfamily K^+ channels in the central nervous system. Mol. Pharmacol. 69, 1673–1683.

Rovira, C., Arbez, N., Mariani, J., 2002. Abeta(25–35) and Abeta(1–40) act on different calcium channels in CA1 hippocampal neurons. Biochem. Biophys. Res. Commun. 296, 1317–1321.

Solntseva, E.I., Bukanova, J.V., Skrebitsky, V.G., 2001. The nootropic drug vinpocetine modulates different types of potassium currents in molluscan neurons. Comp. Biochem. Physiol., Part C Pharmacol. Toxicol. 128, 275–280.

Standridge, J.B., 2002. Pharmacotherapeutic approaches to the treatment of Alzheimer's disease. Clin. Ther. 26, 615–630.

Takada, Y., Yonesawa, A., Kume, T., Katsuki, H., Kaneko, S., Sugimoto, H., Akaike, A., 2003. Nicotinic acetylcholine receptor-mediated neuroprotection by donepezil against glutamate neurotoxicity in rat cortical neurons. J. Pharmacol. Exp. Ther. 306, 772–777.

Thompson, S.H., 1977. Three pharmacologically distinct potassium channels in molluscan neurons. J. Physiol. 265, 465–488.

White, B.H., Kaczmarek, L.B., 1997. Identification of a vesicular pool of calcium channels in the bag cell neurons of *Aplysia californica*. J. Neurosci. 17, 1582–1595.

Xu, C., Qian, C., Zhang, Z., Wu, C., Zhou, P., Liang, X., 1998. Effects of beta-amyloid peptide on transient outward potassium current of acutely dissociated hippocampal neurons in CA1 sector in rats. Chin. Med. J. 111, 492–495.

Yu, B., Hu, G.-Y., 2005. Donepezil blocks voltage-gated ion channels in rat dissociated hippocampal neurons. Eur. J. Pharmacol. 508, 15–21.

Yu, S.P., Farhangrazi, Z.S., Ying, H.S., Yeh, C.H., Choi, D.W., 1998. Enhancement of outward potassium current may participate in beta-amyloid peptide-induced cortical neurons death. Neurobiol. Dis. 5, 81–88.

Zhong, C., Zhang, W., Wang, X., 2002. Effects of donepezil on the delayed rectifier-like potassium current in pyramidal neurons of rat hippocampus and neocortex. Acta Pharm. Sin. 37, 415–418.

Zhou, J., Fu, Y., Tang, X.C., 2001. Huperzine A and donepezil protect rat pheochromocytoma cells against oxygen-glucose deprivation. Neurosci. Lett. 306, 53–56.